Journal of Power Sources 225 (2013) 245–250

Contents lists available at SciVerse ScienceDirect

Journal of Power Sources

journal homepage: www.elsevier.com/locate/jpowsour

# *In-situ* scanning electron microscopy observations of Li plating and stripping reactions at the lithium phosphorus oxynitride glass electrolyte/Cu interface

Fumihiro Sagane [a], Ryosuke Shimokawa [a], Hikaru Sano [b,c], Hikari Sakaebe [b,c], Yasutoshi Iriyama [b,d,*]

[a] Department of Materials Science and Chemical Engineering, Faculty of Engineering, Shizuoka University, 3-5-1 Johoku, Naka-ku, Hamamatsu, Shizuoka 432-8011, Japan
[b] JST, CREST, 5, Sanbancho, Chiyoda-ku, Tokyo 102-0075, Japan
[c] Research Institute for Ubiquitous Energy Devices, National Institute of Advanced Industrial Science and Technology (AIST), 1-8-31 Midorigaoka, Ikeda, Osaka 563-8577, Japan
[d] Department of Materials, Physics and Energy Engineering, Graduate School of Engineering, Nagoya University, Furo-cho, Chikusa-ku, Nagoya 464-8603, Japan

## HIGHLIGHTS

- Li plating–stripping reactions at the LiPON/Cu film interface are observed in-situ by SEM.
- At the Li plating process, nucleation reactions become rate determining step.
- At the stripping process, reaction looks to be governed by lithium diffusivity.
- Plated lithium will react with tiny amount of $H_2O$ and $O_2$ in the SEM chamber.

## ARTICLE INFO

*Article history:*
Received 20 August 2012
Received in revised form
17 September 2012
Accepted 12 October 2012
Available online 26 October 2012

*Keywords:*
Lithium
Anode
All-solid-state battery
*In-situ* SEM
Interface

## ABSTRACT

Morphology variations during electrochemical lithium plating–stripping reactions at the lithium phosphorus oxynitride glass electrolyte (LiPON)/copper current collector (Cu) interface are observed *in-situ* by scanning electron microscopy (SEM). This *in-situ* SEM observation shows dynamically that the plating reactions at 50 μA $cm^{-2}$ distribute initial lithium growth sites sparsely at the LiPON/Cu interface, later, local lithium growth occurs from the pre-plated sites through the Cu film, and finally, most of the precipitated lithium grows to be needle-shape with the height of micron order. This local growth rate attains to be 6.8 mA $cm^{-2}$, about 100 times higher value than applied one. When those precipitated lithium are stripped at 50 μA $cm^{-2}$, core region of each precipitate is mostly stripped but its degree depends on the length of the precipitate. This dependency will arise from the diffusivity of Li. When this stripping current density is increased to 500 μA $cm^{-2}$, the coulomb efficiency is further decreased. *In-situ* SEM observation shows that plated lithium around the interface becomes thin preferentially while that far away from the interface (upper side of plated lithium) remains unchanged. This will isolate most of precipitate lithium from LiPON film electrically, leading to further decreasing of the coulomb efficiency.


## 1. Introduction

All-solid-state batteries (SSBs) using lithium metal (Li) anode are expected to achieve extremely high energy densities with acceptable safety. Inorganic solid electrolyte are non-flammable themselves and also work as the separators against the internal short circuit by dendritic growth of Li. In addition, Li anode has the lowest redox potential with theoretical capacity of 3861 mA h $g^{-1}$, which is ten times larger value than that of commonly-used graphite anode (372 mA h $g^{-1}$). Although the reaction of Li anode in the liquid electrolytes has been widely studied [1–8], electrochemical behavior of Li plating and stripping reactions on inorganic solid electrolytes have hardly understood in detail. This is partly because of less numbers of inorganic solid electrolytes stable with Li.

One of the famous solid electrolytes with stability against lithium metal is lithium phosphorus oxynitride glass electrolyte (LiPON) discovered by Bates et al. [9]. There are many works of thin film batteries (TFBs) using LiPON as the solid electrolyte and Li as the anode material [10–15]. Some of them repeat lithium plating–

* Corresponding author. Department of Materials, Physics and Energy Engineering, Graduate School of Engineering, Nagoya University, Furo-cho, Chikusa-ku, Nagoya 464-8603, Japan. Tel./fax: +81 52 789 3235.
*E-mail address:* iriyama@numse.nagoya-u.ac.jp (Y. Iriyama).

0378-7753/$ – see front matter © 2012 Elsevier B.V. All rights reserved.
http://dx.doi.org/10.1016/j.jpowsour.2012.10.026

stripping reactions for over tens of thousands of cycles without capacity loss. These results suggest that Li plating–stripping reactions occur without any problems in TFBs, but several authors have pointed out another problem during fast lithium plating–stripping process [10,15]. They have assumed the reason to originate from morphology change of Li, but those morphology changes of Li on inorganic solid electrolyte have not been investigated so far. This point has to be clarified well to develop SSBs using Li anode as power sources in large-sized devices, such as electric and hybrid vehicles, requiring high power density.

A powerful technique to investigate such morphology change will be to observe the reaction *in-situ* by scanning electron microscopy (SEM). *In-situ* SEM observations for Li plating process have been already carried out by Neudecker et al. using the TFB of Cu/LiPON/$LiCoO_2$ where $LiCoO_2$ is the Li supplying source [10]. They have clarified that plated lithium react easily with impurity gases, and the resultant dead lithium becomes the source of degradation of Li plating–stripping properties. However, further details on Li plating–stripping morphology have not been investigated. On the other hand, we have found that electrochemically plated Li provides low-resistive Li/LiPON interface than vacuum evaporated Li/LiPON interface, indicating that electrochemically-grown Li anode has advantages to be used in high-power all-solid-state batteries [16]. Thus, it will be meaningful to study on morphology change of electrochemically-grown Li during plating–stripping process in detail.

In the present study, we prepared LiPON film on both sides of mirror-polished $Li^+$ conductive glass-ceramics solid electrolyte sheet (LATP sheet, manufactured by OHARA Inc., Kanagawa, Japan [17]), and assembled Li/LiPON/LATP sheet/LiPON/Cu layer in the SEM. Morphology change during Li plating–stripping process at the LiPON/Cu interface was dynamically observed by *in-situ* SEM.

## 2. Experimental

Schematic image of the *in-situ* SEM observation cell is shown in Fig. 1. The sample used for *in-situ* SEM observation was a two-electrode cell of Li/LiPON/LATP sheet/LiPON/Cu. The LATP sheet basically obtains NASICON-structure with the composition of $Li_{1.4}Ti_2Si_{0.4}P_{2.6}O_{12}$–$AlPO_4$ [18]. Since the LATP sheet is unstable against Li [19], lithium phosphorus oxynitride glass electrolyte ($Li_{3.3}PO_{3.8}N_{0.22}$ (LiPON)) was sputtered on both sides of the LATP sheet by RF magnetron sputtering followed by the preparation conditions reported by Bates et al. [9]. The resultant LATP sheet with LiPON films on both sides will be denoted as LP-LATP sheet in later description. Thin films of Cu (40 nm in thickness, 0.20 $cm^2$ in area) were prepared at first on one side of the LP-LATP sheet by pulsed laser deposition. After that, thin films of Li (4–5 μm in thickness, 0.63 $cm^2$ in area) were deposited on the opposite side of the LP-LATP sheet by vacuum evaporation equipped in glove box. The resultant sample (Cu/LiPON/LATP sheet/LiPON/Li) was mounted in electrochemical SEM holder in argon-filled glove box, where copper plate with a hole was mounted on the Cu film to supply current to the Cu film as shown in Fig. 1. In-plane resistance of the Cu film was too small to be measured by d.c. circuit tester. This electrochemical cell was set into SEM (Keyence VE-9800) without exposing the samples to the air. *In-situ* SEM observation was conducted from top-view through the hole in copper plate. Because of this cell configuration, no pressure was put to the plated lithium during the Li plating–stripping process. As have been reported in the previous paper [16], plated Li grew from the LiPON/Cu film interface toward the Cu film, and the precipitated lithium grew not on the Cu film but burst through the Cu film since the thickness of the Cu film was thin.

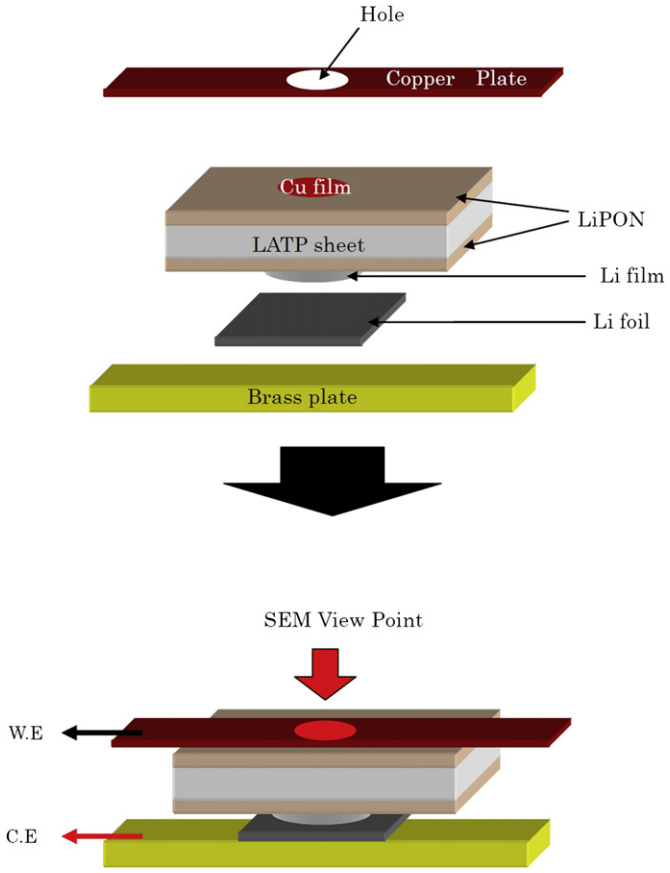


**Fig. 1.** Schematic diagram of an *in-situ* electrochemical scanning electron microscope cell.

Plating of Li were carried out at 50 μA $cm^{-2}$ for 3600 s (0.18 C $cm^{-2}$, 0.25 μm in theoretical thickness), while the stripping ones at 50 μA $cm^{-2}$ or 500 μA $cm^{-2}$ until the voltage attained up to 1.0 V. All electrochemical measurements (Biologic SP-300) were conducted under vacuum condition in the SEM, and Li morphology changes during those plating–stripping reactions were

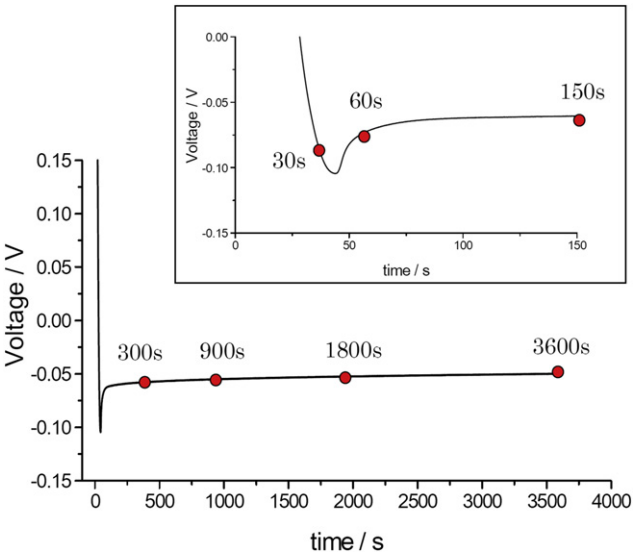


**Fig. 2.** Voltage profile for Li plating reaction on LiPON under the current density of 50 μA $cm^{-2}$. The inset shows the magnified profile around the initial plating reaction. Circles are captured point for in-situ SEM observations, which is shown in Fig. 3.

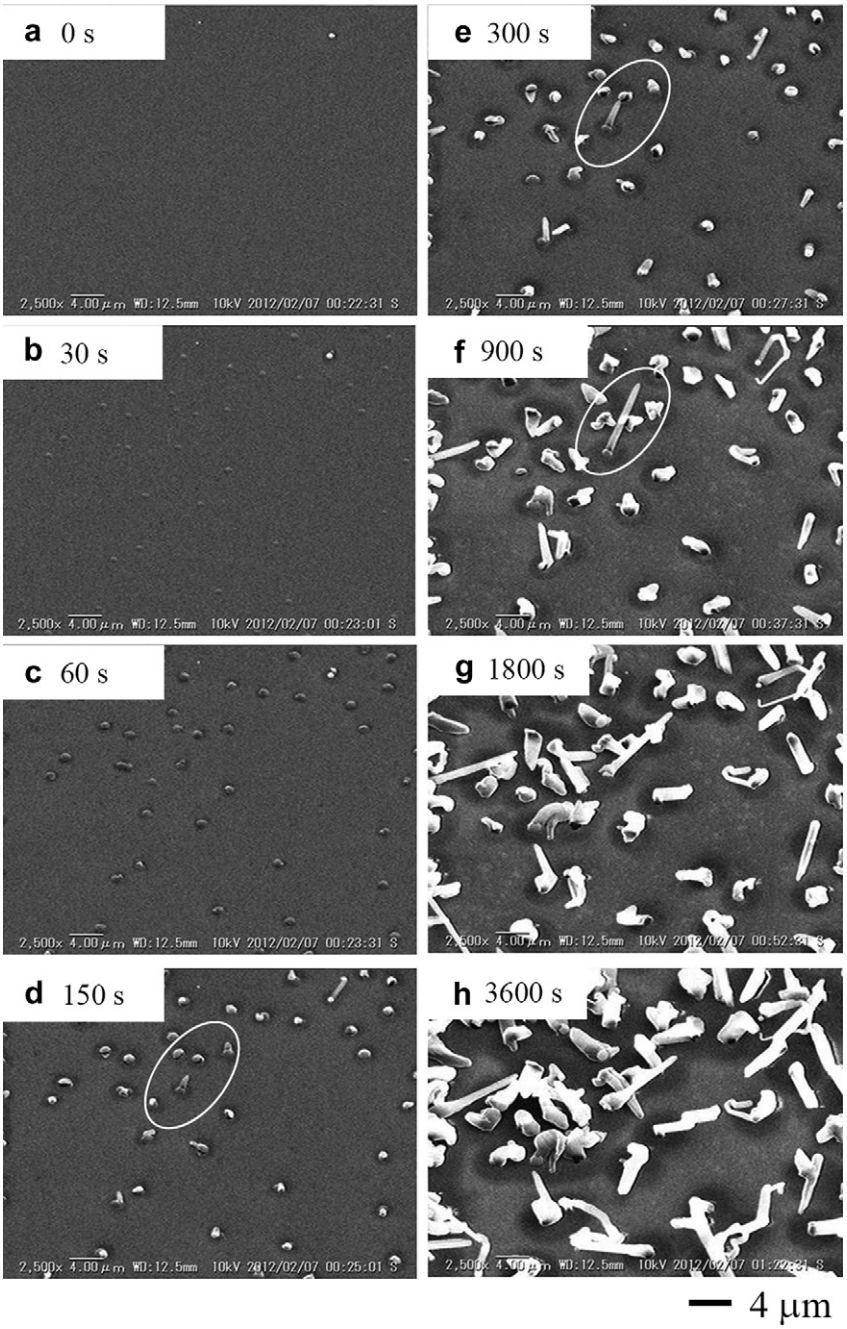


**Fig. 3.** *In-situ* SEM images during Li plating reaction at 50 μA $cm^{-2}$. Those images were captured at (a) 0 s (initial state), (b) 30 s, (c) 60 s, (d) 150 s, (e) 300 s, (f) 900 s, (g)1800 s, and (h) 3600 s, as in Fig. 2.

dynamically observed. Pressure in the SEM chamber was maintained as low as $1 \times 10^{-3}$ Pa during the observations.

## 3. Results and discussion

Voltage profile for Li plating reaction is shown in Fig. 2. The voltage profile shows spike-shaped overvoltage at the initial plating process, followed by gradual voltage increasing with the lithium plating, and finally, the voltage became nearly constant value. This voltage profile was resembled with our past work [16]. Fig. 3(a)–(h) show the SEM snapshots captured at 0 (initial), 30, 60, 150, 300, 900, 1800, and 3600 s, respectively. Initial sample surface looks to be flat (Fig. 3(a)). Small-sized precipitations were observed at the initial potential spike region (30 s, Fig. 3(b)), suggesting that

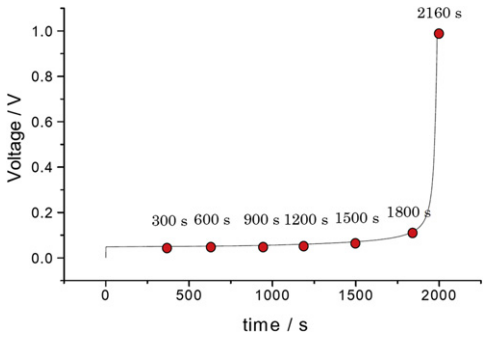


**Fig. 4.** Voltage profile for Li stripping reaction on LiPON at 50 μA $cm^{-2}$. Circles are captured point for in-situ SEM observations, which is shown in Fig. 5.

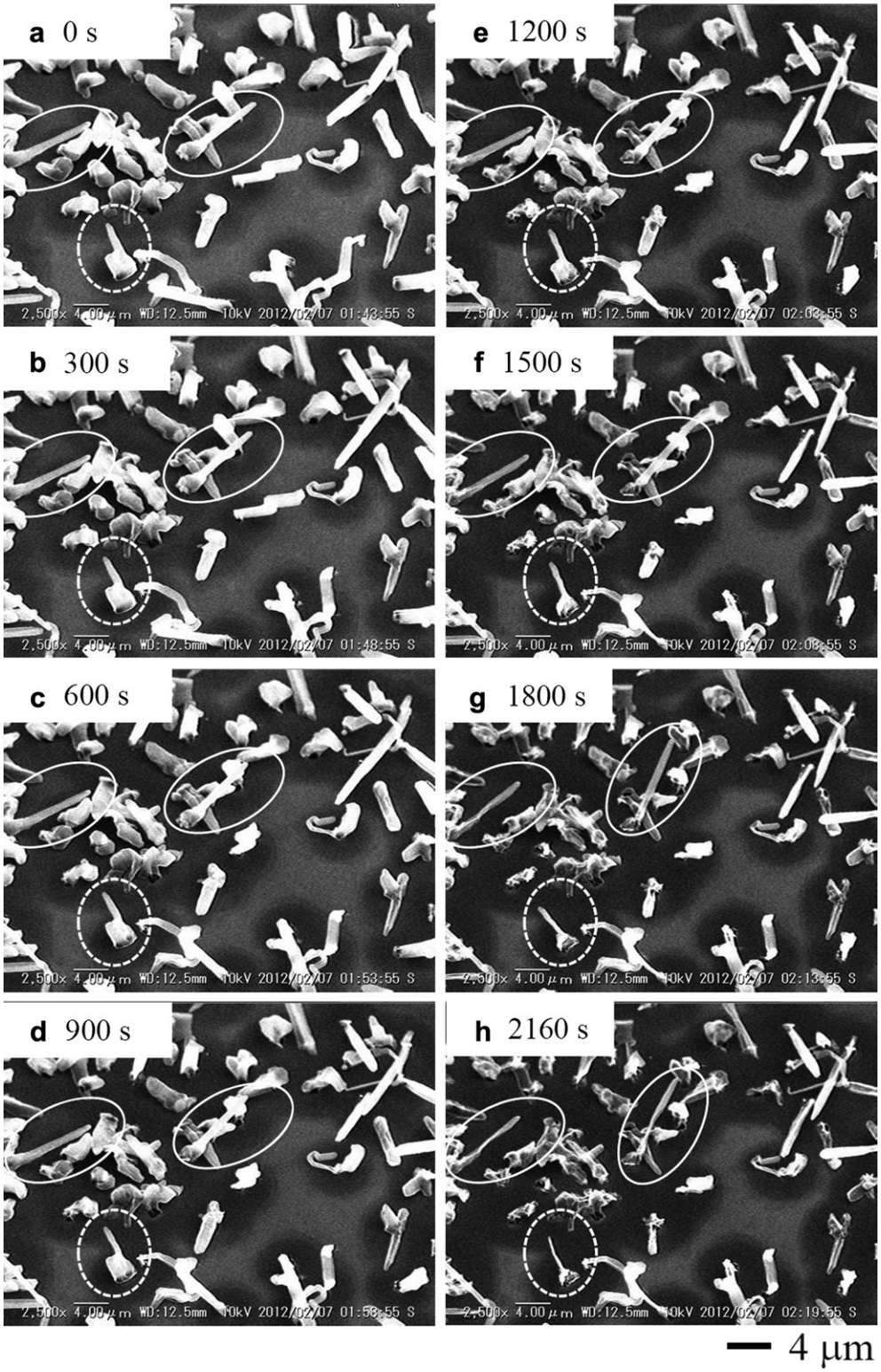


**Fig. 5.** *In-situ* SEM images during Li stripping reaction at 50 μA $cm^{-2}$. Those images were captured at (a) 0 s (initial state; same with Fig. 3(h)), (b) 300 s, (c) 600 s, (d) 900 s, (e) 1200 s, (f) 1500 s, (g) 1800 s, and (h) 2160 s, as in Fig. 4.

initial potential spike is ascribed to the nucleation and growth process. At the voltage increasing region with lithium plating reaction (Fig. 3(c)), lateral growth of the pre-plated precipitation, that is, increasing of the Li/LiPON adhesive region, was observed. Because charge transfer reactions take place preferentially at Li/LiPON interface, this voltage increasing (decreasing of overvoltage) will originate from the reduction of charge transfer resistance at the interface. At the potential stabilized region, plated lithium grew in the vertical direction to the LiPON surface but new precipitated lithium have not been observed so much (Fig. 3(d)–(f)). These results are qualitatively in good agreement with the past works observed by *in-situ* optical microscopy observations [16].

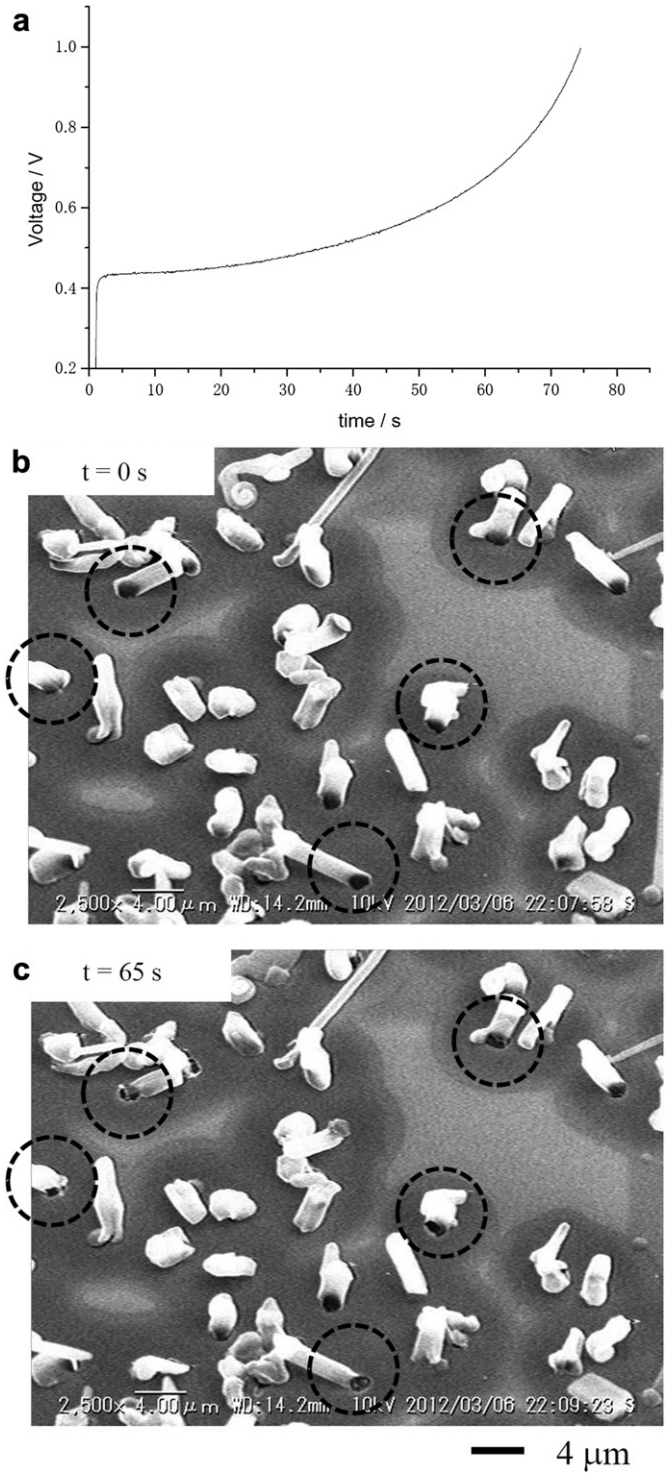


**Fig. 6.** (a) Voltage profile for Li stripping reaction on LiPON at 500 μA cm$^{-2}$. (b, c) *In-situ* SEM images during Li striping process at $t$ = 0 and 65 s, as in (a).

These dynamical observations clarifies that lithium plating reaction occurs preferentially at the pre-plated region, indicating that the net current density at the growth site is larger than the apparent current density. One particular precipitate (surrounded by dotted line in Fig. 3(d)–(f)) was focused on to estimate local lithium growth rate. This precipitate grew continuously to 6.3 μm in height during 750 s (subtraction 150 s in Fig. 3(e) from 900 s in Fig. 3(d)). From the volumetric change and considering the density of Li metal to be 0.534 g cm$^{-3}$, the amount of plated Li during 750 s was calculated. From Faraday's law, the net current density was estimated to be 6.8 mA cm$^{-2}$. This value is about 100 times higher than the apparent current density (50 μA cm$^{-2}$). This indicates that Li plating reaction on the LiPON can occur fast intrinsically.

Fig. 4 shows the voltage profile for Li stripping reaction at 50 μA cm$^{-2}$. The cut-off voltage was achieved before 3600 s and the coulomb efficiency was calculated to be 60%. Snapshots of the SEM captured at 0 (initial, same with Fig. 3(h)), 300, 600, 900, 1200, 1500, 1800, and 2160 s are summarized in Fig. 5(a)–(h), respectively. After the stripping reaction, some residual precipitates were recognized as shown in Fig. 5(h). Looking through Fig. 5(a)–(h), we can find that the morphology change during Li stripping process are greatly different from those for Li plating process (Fig. 3). Precipitated Li seems to deflate and leave a husk of each precipitate. These morphology changes will mean that core region of the precipitates stripped mostly while the surface of the precipitates loses their electrochemical activities. Because *in-situ* formed Li metal is pure Li, it will easily react with residual tiny amount of impurity gases in the vacuum chamber of the SEM, such as $O_2$ and $H_2O$, resulting in the formation of inactive surface film ($Li_2O$, LiOH, etc) [10].

It should be noted that core region of thin precipitated lithium with micron order in length looks to be stripped mostly even additional pressure was not put to each precipitate. Self diffusion coefficient ($D$) of lithium atom in Li has been estimated to be ca. $1 \times 10^{-10}$ cm$^2$ s$^{-1}$ at room temperature [20], thus one-dimensional diffusion length ($(DT)^{1/2}$) for 2000 s will be roughly estimated to be 4.5 μm [21]. When the length of a precipitate is about 5 μm (surrounded by dashed line in Fig. 5(a)–(h)), nearly the same with diffusion length, the precipitate deflated from head to bottom evenly, and only thin surface layer looked to be remained un-stripped. On the other hand, in case of other precipitates with ca. 15 μm in length (surrounded by solid line in Fig. 5(a)–(h)), one order longer than diffusion length, head region looks to be remained unchanged while under the middle region of them deflated as with the shorter ones. This is probably because of the limitation of diffusivity of lithium.

Fig. 6(a) shows the potential profile of stripping reaction at 500 μA cm$^{-2}$. The coulomb efficiency was reduced down to 18%. Fig. 6(b) and (c) show the snapshots of SEM captured at 0 (initial) and 65 s, respectively. Morphology change during stripping process was different from Fig. 5, that is, only around the root of the precipitates became thin as can be recognized in various precipitates surrounded by dotted areas, while upper side of the precipitates remained unchanged. In this case, expected diffusion length for 80 s is estimated to be 1.6 μm, much shorter than the length of many of the precipitates. This means that Li stripping rate will be too high to supply Li from the precipitate. Consequently, electric connection between LiPON and the precipitated Li will be broken, leaving most of the precipitated Li unstripped and then the coulomb efficiency will be decreased. When additional pressure is not put to precipitated lithium, practical current density of dozens mA cm$^{-2}$ at Li stripping process looks to produce an intrinsic serious limitation originating the diffusivity of Li [22].

## 4. Conclusions

Electrochemical lithium plating and stripping reactions at the lithium phosphorus oxynitride glass electrolyte (LiPON)/copper current collector (Cu film) interface were observed *in-situ* by scanning electron microscopy (SEM). This dynamic observation clarifies the variations of lithium plating–stripping morphology. When a current density of 50 μA cm$^{-2}$ was applied for the Li plating reaction, lithium growth sites were distributed sparsely. Local growth rate of a lithium growth site was estimated to be 6.8 mA cm$^{-2}$.

When Li stripping reaction was carried out at low current density (50 μA $cm^{-2}$), core region of each precipitate was mostly stripped but its degree depended on the length of the precipitate. This difference will arise from the diffusivity of Li. Also, inactive lithium looked to be formed on each precipitated Li probably due to the side reactions of the plated pure lithium with residual impurity gases ($H_2O$, $O_2$, etc). These two reasons will reduce the coulomb efficiency to be 60%. On the other hand, when the stripping reaction was carried out at high current density (500 μA $cm^{-2}$), root region of plated lithium became thin preferentially. This situation will produce electrically-isolated precipitate remaining active lithium at its upper region, resulting in further-low coulomb efficiency of 18%. Problems of those lithium plating–stripping reactions at the LiPON/Cu interface were visualized by *in-situ* SEM observations.

## Acknowledgments

The authors acknowledge the financial support by JST-CREST, and also partly by " Promoting Science and Technology System Reform" of JST.

## References

[1] M. Ishikawa, S. Machino, M. Morita, J. Electroanal. Chem. 473 (1999) 279.
[2] K. Morigaki, A. Ohta, J. Power Sources 76 (1998) 159.
[3] J. Yamaki, S. Tobishima, K. Hayashi, K. Saito, Y. Nemoto, M. Arakawa, J. Power Sources 74 (1998) 219.
[4] D. Aurbach, A. Zaban, Y. Ein-Eli, I. Weissman, O. Chusid, B. Markovsky, M. Levi, E. Levi, A. Schechter, E. Granot, J. Power Sources 68 (1997) 91.
[5] M. Arakawa, S. Tobishima, Y. Nemoto, M. Ichimura, J. Yamaki, J. Power Sources 43–44 (1993) 27.
[6] X. Zhang, Y. Li, S. Khan, P. Fedkiw, J. Electrochem. Soc. 151 (2004) A1257.
[7] K. Kanamura, H. Takezawa, S. Shiraishi, Z. Takehara, J. Electrochem. Soc. 144 (1997) 1900.
[8] J. Thevenin, R. Muller, J. Electrochem. Soc. 134 (1987) 273.
[9] J. Bates, N. Dudney, G. Gruzalski, R. Zuhr, A. Choudhury, C. Luck, J. Robertson, Solid State Ionics 53–56 (1992) 647.
[10] B. Neudecker, N. Dudney, J. Bates, J. Electrochem. Soc. 147 (2000) 517.
[11] Y. Iriyama, K. Nishimoto, C. Yada, T. Abe, Z. Ogumi, K. Kikuchi, J. Electrochem. Soc. 153 (2006) A821.
[12] S.-W. Song, H. Choi, H. Park, G. Park, K. Lee, H.-J. Lee, J. Power Sources 195 (2010) 8275.
[13] Y.-I. Jang, N. Dudney, D. Blom, L. Allard, J. Electrochem. Soc. 149 (2002) A1442.
[14] N. Dudney, J. Bates, R. Zuhr, S. Young, J. Robertson, H. Jun, S. Hackney, J. Electrochem. Soc. 146 (1999) 2455.
[15] B. Fleutot, B. Pecquenard, F. Le Cras, B. Delis, H. Martinez, L. Dupont, D. Guy-Bouyssou, J. Power Sources 196 (2011) 10289.
[16] K. Ikeda, K. Okita, H. Sano, F. Sagane, H. Sakaebe, Y. Iriyama, submitted for publication.
[17] http://www.ohara-inc.co.jp/en/product/electronics/licgc.html.
[18] J. Fu, J. Am. Ceram. Soc. 80 (1997) 1901.
[19] Y. Iriyama, C. Yada, T. Abe, Z. Ogumi, K. Kikuchi, Electrochem. Comm. 8 (2006) 1287.
[20] A. Lodding, J. Mundy, A. Ott, Phys. State. Sol. 38 (1970) 559.
[21] Hulmut Mehrer (Ed.), Diffusion in Solids – Fundamentals, Methods, Materials, Diffusion-controlled Processes, Springer, Heidelberg, 2007.
[22] T.R. Jow, C.C. Liang, J. Electrochem. Soc. 130 (1983) 737.